10.4

Predicting Clear-Air Turbulence from Diagnosis of Unbalanced Flow

Steven E. Koch* and Fernando Caracena

NOAA Research–Forecast Systems Lab
Boulder, Colorado

1. INTRODUCTION

Over the last several years, diagnostic algorithms for predicting clear-air turbulence (CAT) have been applied to the Rapid Update Cycle (RUC) model forecasts and incorporated into a fuzzy logic process known as the Integrated Turbulence Forecast Algorithm (ITFA, Sharman et al. 1999). The forecast skill of ITFA and its component algorithms has been evaluated both objectively and by forecasters (e.g. Brown et al. 2000; Mahoney and Brown 2000). These studies show that the best of the algorithms possess rather similar Probability of Detection (POD) curves (Fig. 1), and that there is considerable room for improvement [the optimum scheme would display PODy=1.0 with a value of (1-PODn)=0.0, since PODy (PODn) is the proportion of Yes (No) observations that were correctly forecasted]. Our research indicates that these algorithms also typically predict patterns that are rather similar to one another, and that moderate-or-greater (MOG) pilot reports of turbulence (PIREPS) often fall in the *margins* of the predicted ITFA regions.

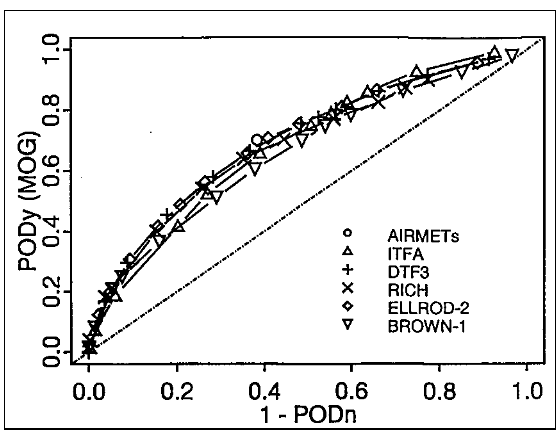

Fig. 1. Plot of skill in 3-h RUC forecasts for ITFA, the best 4 algorithms used by ITFA, and AIRMETs for the period Jan-Mar 2001. Line indicates no skill in forecasts of turbulence. Similar statistical behavior occurs at other forecast times [Brown et al. 2000].

One contributing reason for these seeming deficiencies is that PIREPS are used to steer aircraft from areas where pilots have reported turbulence, resulting in an *apparent* overforecast of the predicted areas. The shortage of PIREP in the center of areas of turbulence makes it very difficult to assess the true performance of turbulence prediction schemes. We suggest that there may be another *dynamical* reason for the suboptimal performance of ITFA algorithms. The best of the ITFA algorithms are fundamentally based on the destabilizing dynamics of vertical wind shear. The Richardson Number Ri (RICH in Fig. 1) varying inversely with the square of the vertical wind shear is one measure of turbulence potential. Another algorithm (BROWN-1) is a simplification of the Ri tendency equation. DTF3 attempts to account for two major sources of turbulent kinetic energy – shear instabilities and vertical momentum flux. ELLROD-2 is simply the product of the magnitude of the vertical wind shear and the combined deformation plus convergence. This latter algorithm assumes that horizontal deformation will produce frontogenesis, resulting in enhanced vertical wind shear needed to maintain thermal wind balance and sufficient to decrease Ri so that shearing instability will be generated. Furthermore, the tilting term, which is the main recognized contributor to upper-level frontogenesis (Keyser and Shapiro 1986), is entirely ignored in ELLROD-2.

We have developed a new turbulence prediction scheme shown schematically in Fig. 2. This scheme is based on the knowledge that mesoscale gravity waves (MGW) displaying wavelengths > 50 km are generated

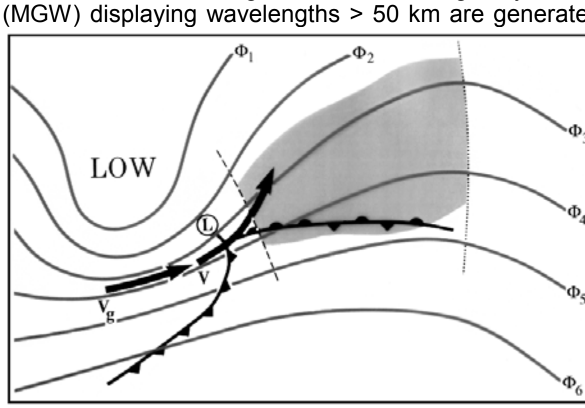

*Fig. 2. Schematic model [Koch and O'Handley (1997)] showing region of MGW activity (shaded) that occurs as a jet streak (**V**) advances ahead of the geostrophic wind maximum (V_g) and approaches an axis of inflection in the upper-level height field (dashed) north of a surface warm or stationary front. Gravity waves are generated near the inflection axis and propagate downstream to the ridge axis (dotted).*

***Corresponding author address**: Steven E. Koch, NOAA/OAR/FSL, FS1, 325 Broadway, Boulder, CO 80305-3328; e-mail < koch@fsl.noaa.gov>

as an unbalanced jet streak propagates toward an inflection axis in the upper-level height field (Uccellini and Koch 1987; Koch and O'Handley 1997), We have diagnosed gravity waves and flow imbalance in several detailed case studies. It will be shown that MOG PIREPs and analyzed MGW consistently occur directly downstream of the region of diagnosed flow imbalance. Evidence is presented that this new scheme not only produces patterns systematically different from the current ITFA algorithms, but that it also predicts turbulence regions missed by those methods.

2. A NEW CAT PREDICTION ALGORITHM

Subjective evaluation of the turbulence prediction algorithms by forecasters at the Aviation Weather Center suggests that MOG turbulence in the winter season is frequently associated with upper troughs and jet streams (Mahoney and Brown 2000). Our own research indicates that MOG PIREPs occur most frequently on days when well-developed cyclonic storms form in areas affecting the major flight routes. In these cases, non-convective turbulence encounters (no lightning nearby) tend to cluster in two areas: the anticyclonic upper-level outflow regions of cyclones, and downstream of the dry slot in the area of strong horizontal deformation surrounding the comma head. This is distinctly different from the behavior of the other ITFA algorithms, which typically maximize in the vicinity of the strongest wind shears associated with the jet stream irrespective of the occurrence of cyclogenesis.

This two-area clustering nature of MOG PIREPs is demonstrated at 1200 UTC 7 February 1999 in Fig. 3. MOG PIREPs are superposed on the corresponding enhanced GOES water vapor image in Fig. 3a, and the corresponding 300-hPa analysis is shown in Fig. 3b. The first cluster of MOG PIREPs stretches from western Wisconsin to eastern Ohio in the anticyclonic upper-level outflow region of a well-developed cyclone centered over southern Illinois. This cluster of turbulence reports is fairly well predicted by the DTF3 algorithm (and ITFA, not shown), though the predicted region (Fig. 3c) is centered northward of the cluster of reports. The second dense MOG PIREPs cluster, over the Ohio Valley region in an arc extending from central Illinois to northern Kentucky, occurs precisely at the tip of the dry slot in the water vapor image. This cluster is essentially missed by the DTF3 and ITFA predictors, but is picked up quite well by our imbalance diagnostic algorithm (Fig. 3d).

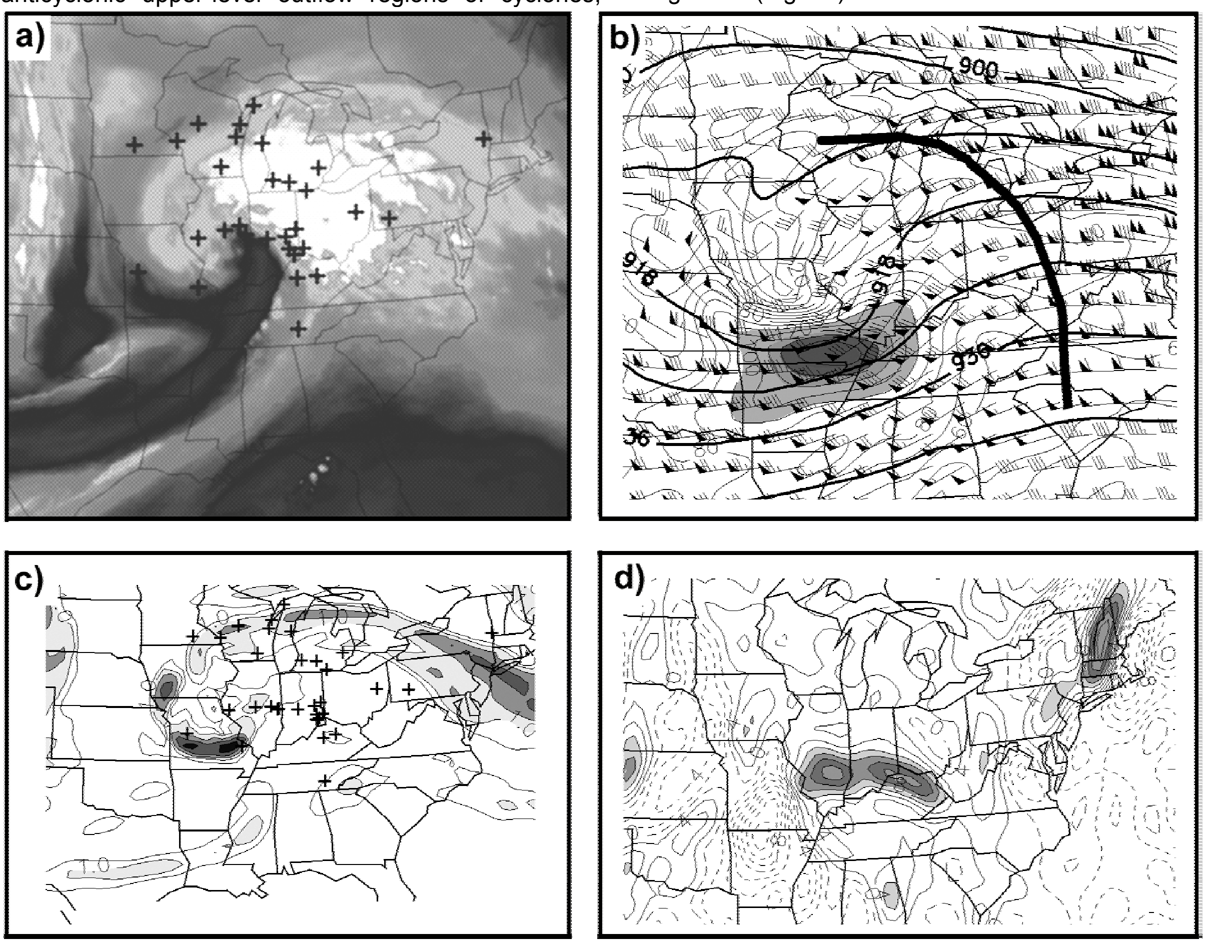

Fig. 3. Analyses and 3-h RUC forecast diagnostics valid at 1200 UTC 7 February 1999: a) enhanced water vapor imagery and time-space converted MOG PIREPs over a ±2h interval, b) heights and winds at 300 hPa, ridge axis (thick curve), and jet isotachs (kt), c) DTF3 prediction of MOG turbulence and PIREPs overlay, and d) unit streamwise advection of the residual of the nonlinear balance equation.

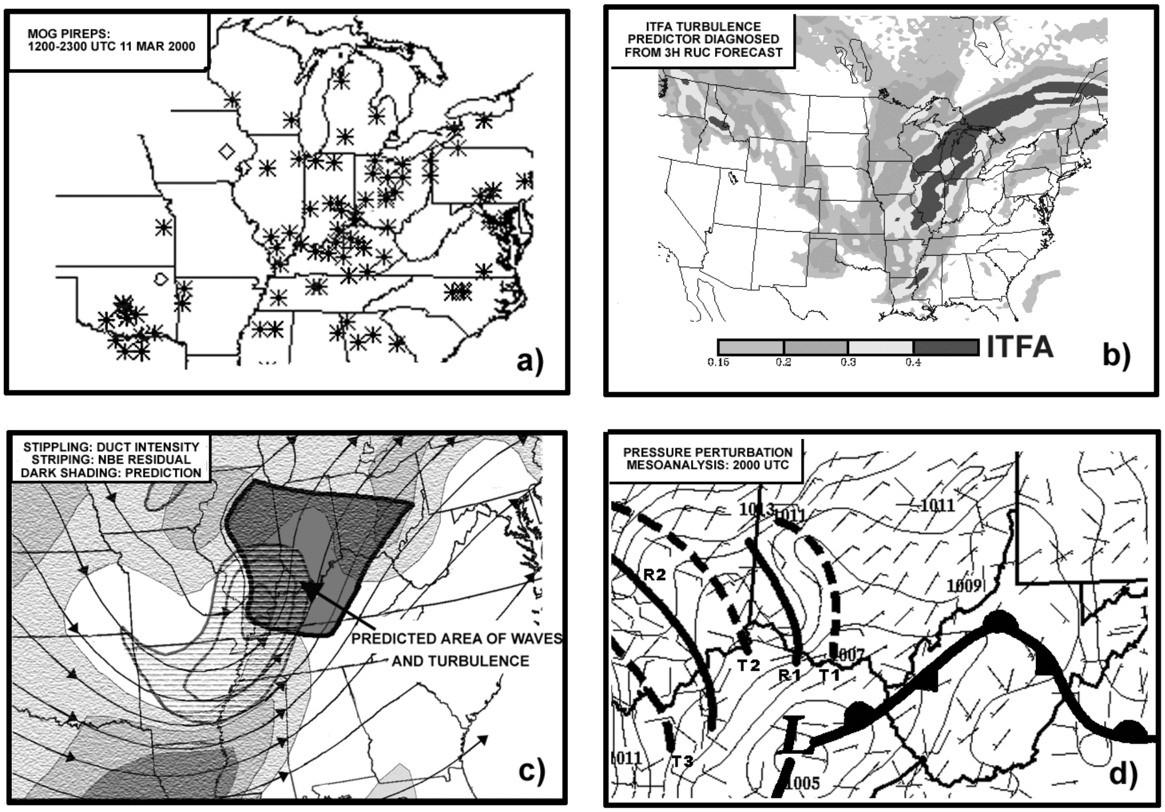

Fig. 4. a) MOG PIREPs for 12-h period beginning at 1200 UTC 11 March 2000, b) ITFA prediction of turbulence from 40-km RUC 3-h forecast valid at 1800 UTC, c) MGW prediction of turbulence and 300-hPa height field from 80-km Eta model 6-h forecast valid at 1800 UTC, and d) diagnosed gravity waves in surface bandpass-filtered mesoanalyses at 2000 UTC [see Koch and Saleeby (2001) for further details about (c) and (d)].

What is meant by "imbalance"? We define the flow to be unbalanced when there is a pronounced residual in the computed sum of the terms in the nonlinear balance equation (NBE), i.e.,

$$R = -\nabla^2\Phi + 2J(u,v) + f\zeta - \beta u \neq 0$$

from the RUC model. Imbalance typically occurs in an area where a jet streak propagates toward the inflection axis in a highly diffluent 300-hPa height field (essentially the same region as that where MGWs typically develop (Fig. 2)). This is occurring over southern Missouri in Fig. 3b; the result is that a large residual in the NBE field is diagnosed over western Kentucky and southeastern Missouri. The turbulence predictor scheme shown in Fig. 3d is calculated as the unit streamwise advection of the NBE residual *R*:

$$\frac{\nabla\Phi \times \mathbf{k}}{|\nabla\Phi|} \bullet \nabla R \, .$$

This field displays a pronounced maximum downstream of *R* stretching from central Illinois to northern Kentucky, coinciding precisely with the second cluster of MOG PIREPs missed by the other ITFA algorithms. The ability of this new scheme, and others based on the concept of unbalanced flow, to add value to the existing ITFA algorithms is characteristic of all the cases we have examined.

3. ALGORITHM TESTING AND MODIFICATION

Further refinement of the forecast region can be obtained by adding the requirement that an efficient wave duct must be present downstream of the region of diagnosed flow imbalance to retard the vertical leakage of wave energy, thus allowing coherent MGW to persist. While mesoscale models like RUC have been found to be useful for diagnosing the flow imbalance regions (Koch and O'Handley 1997), they do not reliably predict the details of the gravity waves themselves (Koch 2001). This next example uses an automated surface mesoanalysis system applied to 5-min ASOS data to analyze *observed* MGWs (Koch and Saleeby 2001), and compares the existence of the diagnosed waves to both PIREPS and various turbulence predictor fields.

A plot of 3-h accumulated MOG PIREPs for the period 0900-1200 UTC 11 March 2000 shows that a coherent area of turbulence centered over the mid-

Mississippi Valley region before 1400 UTC progressed steadily eastward to Ohio and eastern Kentucky in the ensuing 12 h (Fig. 4a). The ITFA product based on a 3-h RUC model forecast valid at 1800 UTC (Fig. 4b) predicts the strongest turbulence to occur in a broad anticyclonic arc extending from eastern Missouri to Quebec, considerably west and north of the actual region of turbulence. Consideration of the NBE residual field (striped shading in Fig. 4c) together with the duct factor field (stippled shading) shows that the region darkly shaded would be where gravity waves and associated turbulence would be predicted. In particular, this region is downstream of the maximum diagnosed imbalance, upstream of a region of large duct factor over the Great Lakes, and limited by the ridge in the 300-hPa height field. This field differs as a potential turbulence predictor from the first case, in that we are here considering the presence of a wave duct as an additional prerequisite for coherent MGW occurrence. The predicted turbulence region encompasses the entire swath of MOG PIREPs over the Ohio Valley missed by ITFA. Finally, the surface mesoanalyses (Fig. 4d) indicate that a very coherent train of gravity waves did indeed propagate from the region of diagnosed imbalance northeastward toward the ridge axis in Ohio and Indiana.

4. CONCLUSIONS AND FUTURE RESEARCH

Our proposed turbulence prediction scheme is based on the concept that mesoscale gravity waves (MGWs) and clear-air turbulence are generated downstream of regions of diagnosed flow imbalance. It appears from the case studies presented here and many others not shown that this scheme adds predictive value to existing approaches, by forecasting distinctly different regions of turbulence missed by other ITFA algorithms.

The residual of the nonlinear balance equation and other methods are being investigated to arrive at the optimum method for diagnosing imbalance. Real-time evaluation of these approaches is being performed in preparation for eventual implementation and full evaluation within ITFA. We should have results of this limited evaluation of the new algorithms in time for the conference.

Nevertheless, our findings raise a very fundamental question: How can CAT be generated by gravity waves with such long wavelengths (>50 km)? The obvious answer is that these waves are not the direct cause of the turbulence, but rather, they are an important predecessor to the generation of Kelvin-Helmholtz instability. Unfortunately, current mesoscale models, while quite useful for diagnosing the conditions in which MGW develop, cannot reliably predict the characteristics of the waves themselves (phase velocity, amplitude, wavelength), not to mention the ability to predict the turbulence intensity. In addition, grid-mean stability, wind shear, and Richardson number do not relate well to the patchy, thin-layered nature of turbulence (Smith and DelGenio 2001).

We hypothesize that clear-air turbulence can develop from MGW as the wave fronts steepen due to nonlinear advection of the dominant wave in a wave packet. Nonlinearity leads to horizontal wavelength shortening, eventual wave breaking, and resultant turbulent kinetic energy generation (Weinstock 1986). Future idealized modeling studies will be performed to develop a basic understanding of the nonlinear scale contraction process by which MGW may steepen and saturate, leading to turbulence production.

5. ACKNOWLEDGMENTS

This research is in response to requirements and funding by the Federal Aviation Administration (FAA). The views expressed are those of the authors and do not necessarily represent the official policy or position of the FAA. Partial funding was also provided by National Science Foundation grant ATM-9700626.

6. REFERENCES

Brown, B. G., et al., 2000: Turbulence algorithm intercomparison: Winter 2000 results. *NOAA Tech. Memo. OAR-FSL-26,* 62 pp.

Keyser, D., and M. A. Shapiro, 1986: A review of the structure and dynamics of upper–level frontal zones. *Mon. Wea. Rev*., **114,** 452–499.

Koch, S. E., 2001: Status report on the predictability of mesoscale gravity waves with numerical weather prediction models. Preprints, *9th Conference on Mesoscale Processes,* Ft. Lauderdale, FL, Amer. Meteor. Soc., 264-268.

____, and C. O'Handley, 1997: Operational forecasting and detection of mesoscale gravity waves. *Wea. and Forecasting*, **12,** 253-281.

________, and S. Saleeby, 2001: An automated system for the analysis of gravity waves and other mesoscale phenomena. *Wea. and Forecasting*, **16,** 661-679.

Mahoney, J. L. and B. G. Brown, 2000: Forecaster assessments of turbulence algorithms: A summary of the Winter 2000 study. *NOAA Tech. Memo. OAR-FSL-27,* 134 pp.

Sharman, R. C., C. Tebaldi, and B. Brown, 1999: An integrated approach to clear-air turbulence forecasting. Preprints, *Eighth Conf. on Aviation, Range, and Aerospace Meteorology*, Dallas, TX, Amer. Meteor. Soc., 68-71.

Smith, S. A., and A. D. DelGenio, 2001: Analysis of aircraft, radiosonde, and radar observations in cirrus clouds during FIRE II: The interactions between environmental structure, turbulence, and cloud microphysical properties. *J. Atmos. Sci.,* **58,**451-461.

Uccellini, L. W., and S. E. Koch, 1987: The synoptic setting and possible energy sources for mesoscale wave disturbances. *Mon. Wea. Rev*.,**115,** 721–729.

Weinstock, J., 1986: Finite amplitude gravity waves: Harmonics, advective steepening and saturation. *J. Atmos. Sci.,* **43,** 688-704.